Chapter 3
Drift Shells and the Second and Third Adiabatic Invariants

3.1 Bounce-Average Drift Velocity and Drift Shells

When a particle bounces along a field line it also drifts perpendicularly to it with an instantaneous drift velocity given by the general expression (2.14). We shall assume this drift to be "slow": during one bounce a particle drifts less than one Larmor radius away from the initial field line, a condition that is usually fulfilled under the adiabatic conditions (2.1), (2.2) or (1.48). In previous sections, we have averaged out the particle's cyclotron motion and worked with a fictitious guiding center particle, with the electromagnetic effects of the periodic cyclotron motion mimicked by the action of an invariant quantity, the magnetic moment $M = T_\perp / B$.[1] There are many situations, especially in radiation belt physics, in which it is not necessary to keep track of the periodic bounce motion up and down the field line, or "bounce phase" (conveniently represented by the field line's arc length s). In such a case, the second periodicity characterized by the bounce period (2.34) can also be averaged out, leaving us with the concept of a "bare" drift motion of the field lines successively occupied by the bouncing guiding center particle, thus generating a surface (Fig. 3.1). We may call the field line along which a particle is bouncing at any given time the *guiding field line*. Each guiding field line is limited by the particle's mirror points. The surface generated by the guiding field line is called a *drift shell*. The mirror points generate the two limiting curves m, m' called *mirror point traces* (or *rings* if the surface is closed). To define the geometric features of a drift shell we need to: (i) identify the initial guiding field line; (ii) find the velocity with which the particle is changing guiding field lines; and (iii) integrate this velocity, thus identifying the subsequent guiding field lines.

[1] In the case of radiation belt particles, it is safe to neglect in (1.6) the drift velocity V_D, therefore it is also safe to replace the GCS velocity $v_\perp{}^*$ in the definition of the magnetic moment (1.24) by the transverse velocity $v_\perp$ in the OFR. We shall do so until further notice.

J.G. Roederer and H. Zhang, *Dynamics of Magnetically Trapped Particles*,
Astrophysics and Space Science Library 403, DOI 10.1007/978-3-642-41530-2_3,

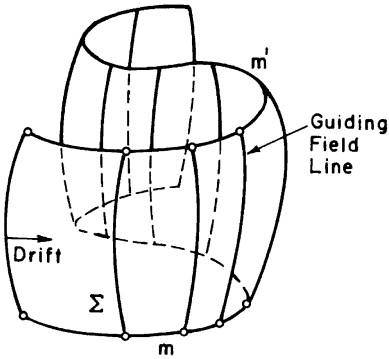

Fig. 3.1 Guiding field lines and generated drift shell Σ

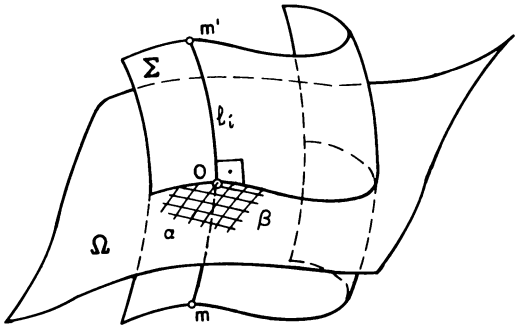

Fig. 3.2 Reference surface and coordinates of the point of a field line

There are many ways of geometrically or analytically identifying a field line in a given magnetic field. The most practical one for our purpose here is the following: Consider a given fixed reference surface $\boldsymbol{\Omega}$ (Fig. 3.2) orthogonal to all field lines; in usual trapping geometries such a surface always exists—the condition is that no field-aligned currents flow (to avoid field line torsion, see Appendix A.1), which we will assume to hold until further notice. Each field line is completely specified by the position of its intersection point O on the reference surface $\boldsymbol{\Omega}$. If α, β is a curvilinear coordinate system on $\boldsymbol{\Omega}$, the two scalars α, β specify a given field line ℓ (Fig. 3.2).[2] We already mentioned in the previous section that a particularly convenient referencein the geomagnetic field is the minimum-B equatorial surface

[2]For a divergence-free vector field like the magnetic field, the so-called *Euler coordinates* (e.g., [1, 2]) can be used, defined as $\alpha = \alpha(\boldsymbol{r}, t)$, $\beta = \beta(\boldsymbol{r}, t)$, with the property vector potential $\boldsymbol{A} = \alpha \boldsymbol{\nabla} \beta$ and therefore $\boldsymbol{B} = \boldsymbol{\nabla} \alpha \times \boldsymbol{\nabla} \beta$. A magnetic field line ℓ is defined by $\alpha = \alpha_\ell = \text{const.}$, $\beta = \beta_\ell = \text{const.}$; the third coordinate in the Euler system can be the field line arc length s, a curvilinear distance to some reference surface $\perp \boldsymbol{B}$.

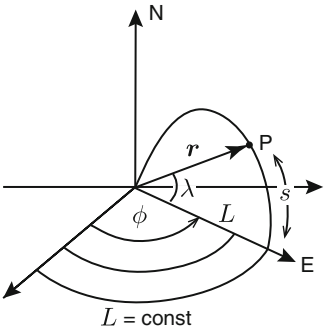

Fig. 3.3 Euler coordinates L, ϕ and s for a dipole field

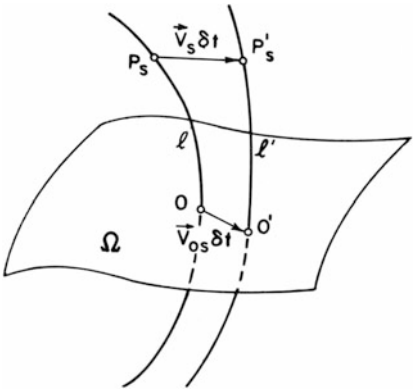

Fig. 3.4 Instantaneous and bounce-average drift velocities

(locus of the minimum-B points of all field lines and, therefore, also locus of all bounce motion equilibrium points). In the case of a pure dipole (or any field with north—south symmetry) it is a plane, in which case the two most convenient α, β parameters are proportional to the polar coordinates (radius vector r_0 and longitude ϕ_0) of the equatorial point E of the field line (see Fig. 3.3): $\alpha \sim r_0$ and $\beta \sim \phi_0$. In a dipole field, r_0 can be thought of as a 3-D scalar function $L = L(\boldsymbol{r})$, namely the modulus of the radius vector of the minimum-B point of a field line traced through *that* point $\boldsymbol{r}$. All points of a dipole field line have the same L-value (for the relations between L, s and $\boldsymbol{r}, \lambda$ see Sect. 3.4). In the general case of a more complex field (e.g., the field in a mirror machine or field lines near the dayside boundary of the magnetosphere) there may be more than one minimum-B point along one field line and the equatorial surface may have several branches (e.g., [3]). We shall not consider such a complication. As a guiding center particle bounces and drifts occupying successive guiding field lines, the intersection point O with the reference surface moves along that surface. We can introduce what is called the particle's *bounce-average drift velocity*. Refer to Fig. 3.4: if $\boldsymbol{V}_s$ is the actual, instantaneous drift velocity of the particle while its guiding center is passing through a point P at arc position s_p, the displacement of point O associated with the instantaneous

displacement $\boldsymbol{V}_s\delta t$ (where $\delta t < \tau_c$) will be given by $\overrightarrow{\boldsymbol{OO'}}$ ($|OO'| \ll \rho_L$). The point O′ is obtained by tracing the field line ℓ' that goes through P′ down to the reference surface Ω. The associated drift velocity $\boldsymbol{V}_{0s} = \overrightarrow{\boldsymbol{OO'}}/\delta t$ on the reference surface is related to the actual local drift velocity $\boldsymbol{V}_s$ through a transformation that only depends on the actual field geometry (in the case of a dipole field, it is $V_{0s} = \cos^{-3}\lambda V_s$, where λ is the latitude of point P). The *bounce-average drift velocity* of O will then be given by:

$$\langle \boldsymbol{V}_0 \rangle = \frac{1}{\tau_b}\int_0^{\tau_b} \boldsymbol{V}_{0s} dt = \frac{2}{\tau_b}\int_{s'_m}^{s_m} \boldsymbol{V}_{0s}\frac{ds}{v_\parallel} \tag{3.1}$$

Let us consider the case of a static magnetic field without field-aligned currents, in which a trapped particle is subjected to an electrostatic field always perpendicular to $\boldsymbol{B}$. When the guiding center particle is at position s and the pitch angle cosine of the original particle is μ_s, we have for the local drift velocity, taking into account (1.34), (2.17) and (1.14):

$$\boldsymbol{V}_s = \frac{\boldsymbol{E}_s \times \boldsymbol{B}_s}{{B_s}^2} + \frac{m{v_s}^2}{2q{B_s}^3}(1+{\mu_s}^2)\boldsymbol{B}_s \times \boldsymbol{\nabla}_\perp B_s \tag{3.2}$$

Based on purely field-geometric arguments we prove in Appendix A.2 that the bounce-average (3.1) of expression (3.2) is given by

$$\langle \boldsymbol{V}_0 \rangle = \frac{\boldsymbol{\nabla}_0 J \times \boldsymbol{e}_0}{q\tau_b B_0} \tag{3.3}$$

in which

$$J = \oint p_\parallel ds = m\oint v\,\mu\, ds \tag{3.4}$$

is an integral taken along the guiding field line for a complete bounce cycle ($\oint = 2\int_{s'_m}^{s_m}$). In the specific case of *equipotential field lines*, v is constant during one bounce, and taking into account the definition of the purely field-geometric quantity I (2.37),

$$J = 2pI \tag{3.5}$$

In Appendix A.2 we also show that for equipotential field lines (p is constant along a field line, but not across it!):

$$\boldsymbol{\nabla}_0 J = 2p\boldsymbol{\nabla}_0 I + q\,\tau_b\,\boldsymbol{E}_0 \tag{3.6}$$

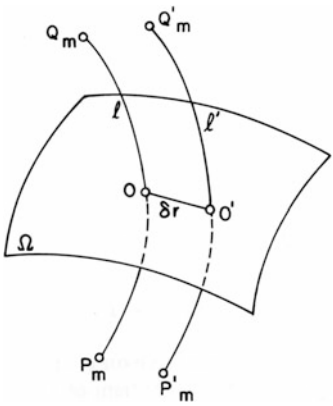

Fig. 3.5 Field line configuration for the definition of the gradient of J or I

With this relation, (3.3) becomes, replacing τ_b with $2S_b/v$:

$$\langle \boldsymbol{V}_0 \rangle = \frac{\boldsymbol{E}_0 \times \boldsymbol{B}_0}{{B_0}^2} + \frac{mv^2}{qS_b B_0} \nabla_0 I \times \boldsymbol{e}_0 \tag{3.7}$$

All quantities in (3.3) and (3.7) are defined at the reference point O. These expressions thus represent the average drift velocity *of the reference point* of the guiding field line. In principle, since the surface Ω could be any surface normal to the field lines, that reference point could be *any* point of a field line between the particle's mirror points. Choosing for instance one of the latter, (3.7) would then become the average drift velocity of one of the particle's mirror points.

Although everybody knows how a gradient is defined, it is prudent to give the "recipe" for the numerical calculation of the gradients of J or I in the above expressions (see Fig. 3.5). It consists of the following steps: (i) Consider a particle of given magnetic moment (or kinetic energy) and pitch angle, for which $\nabla_0 J$ (or $\nabla_0 I$) is wanted (Ω is a reference surface perpendicular to all field lines). (ii) Compute numerically the integral (3.4) (or (2.37)) for the guiding field line between the mirror points (given through M and α). (iii) Take a neighboring field line ℓ' and compute J or I between the mirror points that would result for a particle with the *same* magnetic moment and total energy placed on that field line (same B_m if there are no forces). (iv) Form the ratio $\delta J/\delta r = (J' - J)/|OO'|$. (v) Repeat the process for other neighboring field lines (chosen in some "logical" way) until the one for which $|\delta J/\delta r|$ is maximum is found. The direction of $\nabla_0 J$ will be that of the vector $\overrightarrow{OO'}$; its magnitude will be the limit of $\delta J/\delta r$ for $\delta r \to 0$. Notice carefully that just like $\langle \boldsymbol{V}_0 \rangle$, $\nabla_0 J$ or $\nabla_0 I$ depend on the reference surface (point O).

With (3.7) we can find specific adiabatic conditions required for the validity of all preceding definitions. We stated before that the drift displacement of the reference

point during one bounce should be much less than one typical Larmor radius (1.22):

$$\delta_0 = \langle V_0 \rangle \tau_b = \frac{E_0}{B_0}\tau_b + \frac{2p\nabla_0 I}{qB_0} \ll \rho_C$$

which leads to the simultaneously required conditions

$$V_E = E_0/B_0 \ll \frac{\rho_C}{\tau_b} \sim v\frac{\tau_C}{\tau_b} \quad \text{and} \quad \nabla_0 I \ll 1 \tag{3.8}$$

Given a particle injected along an initial field line, one can find the intersection with the reference surface Ω of all subsequent guiding field lines by integration of (3.3) or (3.7) along that intersection curve. The full drift shell is then determined by tracing the field lines through all reference points up and down to the local mirror points defined by the conservation of M and $\mathfrak{E}$. This may be quite lengthy; in many practical applications one just wants to find the guiding field line at some given longitude far away from the initial field line, without having to trace the intermediate drift track. To accomplish that, we can use the fundamental property of J (or I for a static magnetic field without external forces) as a second adiabatic invariant and search for the particle's mirror point at the wanted longitude—as we shall show in the next section.

3.2 The Second Adiabatic Invariant

The quantity J (3.4) is an adiabatic invariant conserved during the drift of a guiding center particle in a trapping geometry,[3] provided adiabatic conditions (2.1), (2.2) and (3.8) apply. This conservation theorem follows at once from (3.3): since $\langle \boldsymbol{V}_0 \rangle$ is of the form "scalar times $(\boldsymbol{\nabla}_0 J \times \boldsymbol{e})$", the drift is in a direction *normal* to the gradient of J, so that on the following guiding field lines the value of J will remain constant. Remember that J must be computed for constant M and $\mathfrak{E}$, and that the mirror points must be determined through (2.38) or (2.43).

Let us first consider the case in which *no external forces are acting and the magnetic field is static*. Conservation of J implies that of the field-geometric integral I (2.37). Furthermore, since the potential energy W and the particle's kinetic energy T are constant in this case, the conservation of magnetic moment $M = T_\perp/B = T/B_m$ leads to the conservation of mirror field intensity. In summary, we have

[3] Going back to the footnote on page 10 concerning canonical path integrals, we can consider the bounce motion as a cyclic motion, with the field line arc length s as the variable. In that case, $J_b = \oint (\boldsymbol{p} + q\boldsymbol{A}) \cdot \boldsymbol{ds}$. This time the cyclic orbit (up and down the field line) encompasses *zero* magnetic flux; therefore only the first term subsists and is equal to $J_b = \oint \boldsymbol{p} \cdot \boldsymbol{ds}$, equal precisely to what we defined as the second invariant J, which is therefore adiabatically constant.

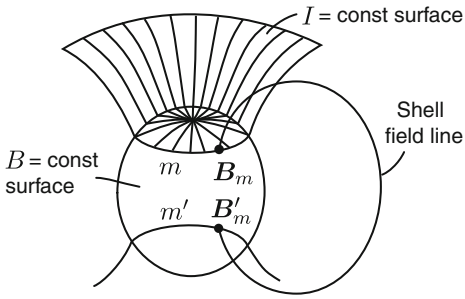

Fig. 3.6 Sketch of the geometric relations between B = const., I = const. and drift shell surfaces

$$I = \text{const.} \tag{3.9}$$

$$B_m = \text{const.} \tag{3.10}$$

These relations define the drift shell of a particle as the surface generated by all field lines that pass through the intersection curves m, m' (mirror traces) of the corresponding I = const. and B_m = const. surfaces (Fig. 3.6). The values of I and B_m are determined by (2.37) and (2.33), respectively, which in turn are calculated for the initial position and pitch angle of the particle in question. In all this, the second invariant has to be envisioned as a *scalar function of space* $I = I(\boldsymbol{r})$ defined by the I-value of a particle mirroring *at that point* $\boldsymbol{r}$. Relations (3.9) and (3.10) tell us that for a static case in absence of external forces, drift shells are independent of a particle's mass, charge and energy: they only depend on the particle's initial guiding center position and pitch angle. Note carefully that the constancy of I and B_m for a drifting particle does not imply constancy of the bounce path (2.35) or bounce-average drift velocity, which in this special case is

$$\langle \boldsymbol{V}_0 \rangle = \frac{mv^2}{qS_b B_0} \nabla_0 I \times \boldsymbol{e}_0 \tag{3.11}$$

In a pure dipole magnetic field we do not have to invoke the conservation of the second invariant I: for reasons of azimuthal and N-S symmetry, it is enough to determine the field line (given by the parameter L, see Fig. 3.3) through the initial position and the mirror point B_m given by (2.33), and then rotate the portion of field line between conjugate mirror points around the dipole axis.

Unfortunately, for any other field geometry with no symmetries, no simple analytical expressions exist that can be used to determine the drift shell field lines of a trapped particle. The integral function $I = I(\boldsymbol{r})$ must be determined *numerically*, using a mathematical model (numerical or analytical) of the magnetic field $\boldsymbol{B} = \boldsymbol{B}(\boldsymbol{r})$. Given a particle injected with a certain pitch angle at a point of some initial field line, the computational procedure to find the particle's shell field line at any other longitude is then as follows. First, once you have the initial point B value, determine B_m and compute I by tracing the field line between the two initial conjugate mirror points. Then go to the wanted longitude and by picking different points for which $B = B_m$ (see Fig. 3.6) instruct the computer to find by an iterative method *that* field line for which the value of (2.37) between mirror

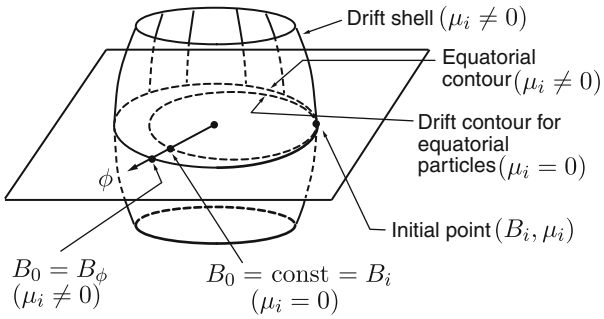

Fig. 3.7 Schematic view of the drift contour of an equatorial particle ($\mu_{0i} = \cos\ \alpha_{oi} = 0$) and of the drift shell of a $\mu_{0i} \neq 0$ particle, in an azimuthally asymmetric field

points is equal to the initial value $I\pm$ prefixed error. If no such field line can be found, it means that on that meridian no trapping is possible for a particle of the prescribed I, B_m values—the particle must have left its trapping region before drifting to the longitude in question. Notice that in this way we indeed can find shell field lines at arbitrary longitudes *without* having to proceed in small longitudinal drift steps from the initial guiding field line. Of course, if the drift time from initial to final longitude is wanted, it is necessary to integrate (3.11): $\tau_D = \oint \langle V_0 \rangle^{-1} d\ell$.

For particles mirroring close to the equator, we can use an expansion of $B(s)$ similar to the one leading to (2.39) and (2.40) in the definition of I (2.37), to obtain to first order:

$$I \cong \frac{\pi}{\sqrt{2}} \left(\frac{B_m}{a_0}\right)^{1/2} \left(1 - \frac{B_0}{B_m}\right) \cong \frac{\pi}{\sqrt{2}} \left(\frac{B_0}{a_0}\right)^{1/2} \mu_0^2 \tag{3.12}$$

where $a_0 = \partial^2 B/\partial s^2$, B_0 and μ_0 are taken at the minimum-B point. This expression and the constancy of B_m and I lead us to an analytical expression to first order in ${\mu_0}^2$ of the equatorial trace (in terms of equatorial B-values) of a drift shell for near-90° pitch angle particles (Fig. 3.7):

$$B_0(\phi) = B_{0i} \left[1 - \left(\frac{a_0(\phi)}{a_{0i}}\right)^{1/2} \mu_{0i}^2\right] \tag{3.13}$$

For $\mu_{0i} \neq 0$, the second derivative $a_0(\phi) = \partial^2 B/\partial s^2|_{0\phi}$ only needs to be evaluated at the $B_0(\phi) = B_{0i} = \text{const.}$ contour (see Fig. 3.7), since under the present approximation μ_{0i}^2 is very small. Clearly, for equatorial 90° pitch angle particles as well as for azimuthally symmetric fields, the equation of the shell intersection is $B_0(\phi) = B_{0i} = \text{const.}$, as we have seen for a special case in Sect. 1.6. The longitudinal variation of $B_0(\phi)$, i.e., the azimuthal distortion of the drift shell, is determined by the longitudinal variation of $a_0(\phi)$: in all azimuthally asymmetric fields, particles with different initial pitch angles will generate different drift shells. This is called shell-splitting and will be discussed in more general terms and without pitch angle restrictions in the next section.

We end this section with a return to the more realistic situation of particle trapping in a static magnetic field *under the action of external forces perpendicular to the magnetic field lines* (i.e., still excluding field-aligned forces). Assuming that the external force derives from an electrostatic potential $\boldsymbol{F} = -q\nabla V(\boldsymbol{r})$, field lines will be equipotentials, each with a potential which we denote by $V_0(\boldsymbol{r}_0)$, the potential of its intersection with the minimum-B surface. Under such conditions, the integral I (2.37) will no longer be an adiabatic invariant; however, we can easily derive one, which we call K, by combining the invariance of the magnetic moment M (1.26) with (3.5):

$$K = \frac{J}{2\sqrt{2mM}} = I\sqrt{B_m} = \int_{s'_m}^{s_m} (B_m - B(s))^{1/2}\, ds = \text{const.} \tag{3.14}$$

This quantity still is "purely field-geometric" like I, independent of the particle—but only to a certain point: the limits of the integral in (3.14) are not constant (invariants) like those in (3.9), but depend on the initial mirror points and the local kinetic energy of the particle, which is no longer constant. The conservation of total energy $\mathfrak{E}$ and the adiabatic constancy of M and K yield the following equations that allow us to determine a particle's guiding field line at any longitude ϕ, thus if we wish, the entire drift shell (subindex i stands for initial):

$$\mathfrak{E} = T(\phi) + qV(\phi) = T_i + qV_i = \text{const.} \tag{3.15}$$

$$M = \frac{\mathfrak{E} - qV(\phi)}{B_m(\phi)} = \frac{T_i}{B_{mi}} = \text{const.} \tag{3.16}$$

$$K = I_\phi\sqrt{B_m(\phi)} = I_i\sqrt{B_{mi}} = \text{const.} \tag{3.17}$$

The numerical determination of drift shells for given models of $\boldsymbol{B}(\boldsymbol{r})$ and $V_0(\boldsymbol{r}_0)$ is qualitatively similar to the procedures given above for a magnetic field in absence of an electrostatic field, except that now the mirror point B-values are energy dependent and have to be recalculated for each field line using (3.16), and that at the wanted longitude the iterative process must zero-in on a prefixed K value ($\pm$ prefixed error) instead of I.

3.3 Shell Splitting and Pseudo-trapping

It is important to analyze in general terms some characteristic geometric properties of trapped particle drift shells in typical asymmetric magnetospheric field models (in absence of electric fields). Take a particle that starts at a given longitude ϕ_0, circling and bouncing about a guiding field line between conjugate mirror points at a field value B_m. The integral (2.37) has a value I. This means that when drifting through any other longitude, for example 180° away, this particle will bounce along a field line that passes through the intersection of the corresponding I = const. and B_m = const. surfaces (Fig. 3.8). Now take a particle which starts on the *same* initial

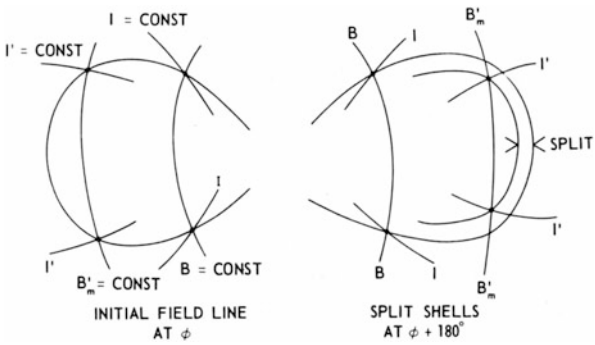

Fig. 3.8 Geometric depiction of shell splitting in an asymmetric field

field line but mirrors at a lower value, $B'_m < B_m$. Its integral I' will also be smaller, $I' < I$. After a 180° drift this second particle will be bouncing along a field line that passes through the intersection of the surfaces $I' = \text{const.}$ and $B'_m = \text{const.}$ *Only* in the case of perfect azimuthal symmetry (as in a pure dipole) will these surfaces intersect *exactly* on the same field line as that of the first particle, and thus the shells of both particles will be coincident. This latter case is called *shell degeneracy*. In the general case, however, as we already have seen for the near-equatorial case in (3.13), particles starting on a common field line at a given longitude will populate *different* shells according to their initial mirror point fields or, which is equivalent, according to their initial equatorial pitch angles. This effect is called *shell splitting* [4]. Of course, all these drift shells will be tangent to each other on the initial field line.

Let us analyze a quantitative example. In doing so, we will not insist in the accuracy of the magnetospheric field model used; the principal conclusions depend on broad features, common to all specific models. We will use some of the old, analytically simple and computationally fast models of the 1960s and 1970s, such as the Mead-Williams model [5]. Figure 3.9 shows how particles, starting from a common field line in the *noon* meridian with equatorial pitch angle cosines μ_0 of 0.2, 0.4, 0.6, 0.8 and nearly 1 (mirroring close to the Earth's surface), do indeed drift on different shells which intersect the midnight meridian along different field lines. The dots represent the particle's mirror points. Curves giving the position of mirror points for constant equatorial pitch angles are shown for comparison (in a dipole field, they should be constant latitude lines, Appendix A.2). Notice the change (decrease) in equatorial pitch angle for the same particle when it drifts from noon to midnight. Figure 3.10 depicts the same features for particles starting on a common field line in the *midnight* meridian. In this case, again, the equatorial pitch angle changes considerably when the particle drifts to the opposite meridian (increasing at noon). Notice from these two examples that, as equatorial pitch angles increase, shell splitting is directed radially earthwards for particles starting on the same field line at noon, and radially outwards for particles starting on a common field line at midnight. Furthermore, shell splitting is maximum for particles mirroring close to the equator. The more distorted the magnetospheric field (compared to a dipole-like field), the more pronounced these effects are.

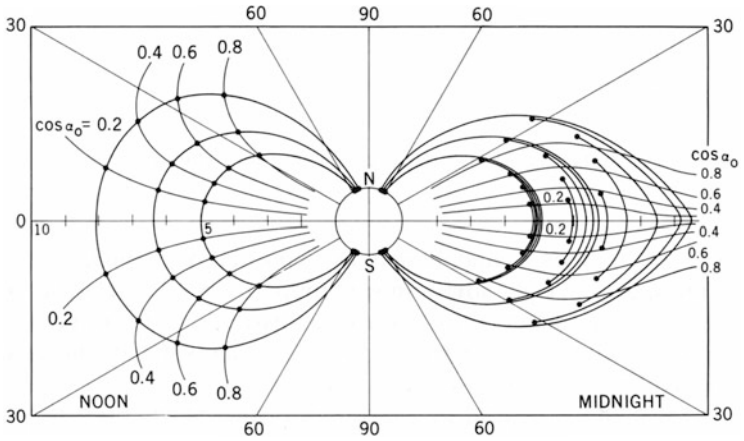

Fig. 3.9 Computed shell splitting for particles starting on common field lines in the noon meridian (a simple magnetospheric field model was used [6]). *Dots* represent particles' mirror points. *Curves* giving the position of mirror points for constant equatorial pitch angle α_0 are shown

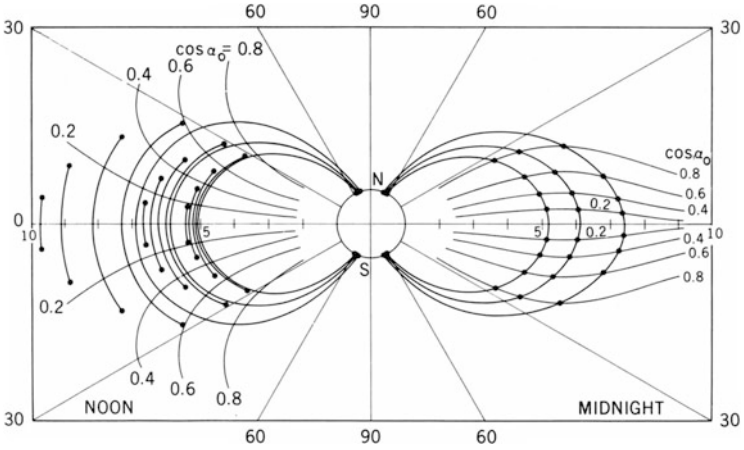

Fig. 3.10 Same as Fig. 3.9, for particles starting on common field lines in the midnight meridian

An interesting feature (not shown in Figs. 3.9 and 3.10) arises with particles of equatorial pitch angles smaller than ∼45°–50° ($\mu_0 \sim 0.45$), i.e., mirroring closer and closer to the earth. For that "magic" pitch angle[4] drift shells are azimuthally symmetric (like in a dipole); as the pitch angle decreases further (μ_0 increases),

[4]Magic, because it is practically independent of magnetospheric field model details and of the radial distance to the field line's equatorial point!

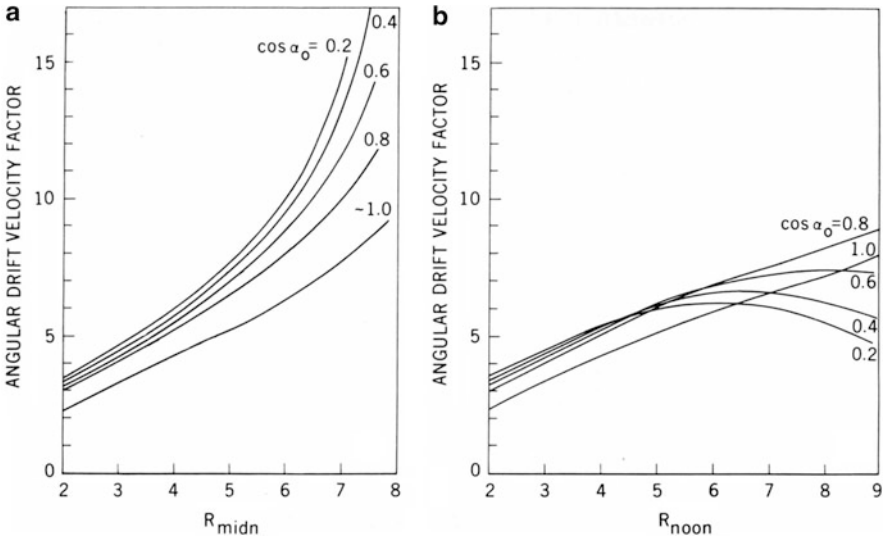

Fig. 3.11 Value of the geometric factors intervening in the bounce-average angular drift velocity as a function of the equatorial distance of the corresponding field line, for different pitch angles and or midnight and noon, respectively. To obtain drift velocities in degrees/sec, multiply the above values by the factor $2.321 \times 10^{-2}(\gamma^2 - 1)/\gamma$ times rest mass (in electron masses)

shell splitting, while small, reverses its sense: particles on the same field line at midnight are found on field lines *closer* to the earth at noon, and the opposite for particles that mirror on the same field line at noon. Looking at Figs. 3.9 and 3.10, we realize that the dependence of shell splitting on the initial pitch angle is most pronounced for near equatorial particles ($\mu_0^2 \ll 1$). For this reason, the variability along a constant-B contour of the ratio $a(\phi)/a_0$ in (3.13) is a good indicator of the "strength" of shell splitting in a given magnetospheric field model.

Concerning the bounce-average drift velocity (3.11), numerical calculations also reveal a considerable local-time (longitudinal) dependence for any azimuthally asymmetric field, as we already have seen in the case of equatorial particles (Sect. 1.6). The particle-independent geometric factors appearing in (3.11) are represented in Fig. 3.11 as a function of the equatorial distance of the corresponding field line, for different pitch angles and for the midnight and noon meridians, respectively. For better understanding *angular* drift factors are shown. For radial distances $\lesssim 3\,R_E$ we observe a dipolar dependence. Beyond $\sim 3\,R_E$ there is a considerable departure. Angular drift velocities on the night side are appreciably higher than on the dayside. The peculiar inversion of the pitch angle dependence occurring on the dayside is due to the fact that particles mirroring at low latitudes experience on the average during their bounce a greatly reduced field gradient, whereas those mirroring at high latitudes spend a larger fraction of their bounce-time in a dipole-like field and hence drift faster. A closer inspection of the local-time dependence of the bounce-average drift velocity (not shown) shows that a given particle trapped in the outer magnetosphere ($r \gtrsim 6\,R_E$) spends from 2/3 to 3/4 of its time on the dayside. In other words, there is always a higher probability of

finding a trapped particle on the dayside than on the night side. This has important consequences for trapped particle diffusion.

When a field line has its equatorial point beyond about $8\,R_E$, a fraction of the particles mirroring on it are *pseudo-trapped* or *quasi-trapped*, being unable to complete a drift around the Earth. In particular, as we already have seen for equatorial particles in Sect. 1.6, particles mirroring at midnight close to the minimum-B surface, will abandon the magnetosphere through the boundary near dawn or dusk (depending on their charge, i.e., the direction of drift) before reaching the noon meridian. On the other hand, particles mirroring at high latitudes on the dayside will run into the magnetospheric tail before reaching the midnight meridian. Figure 3.12 shows computed limits between stable trapping and quasi-trapping regions on the noon-midnight meridian. At other local times one quasi-trapping region disappears at the expense of the growth of the other. The calculation of open drift shells in the pseudo-trapping regions using the adiabatic invariants is cumbersome; recently, full particle orbits in the high-latitude pseudo-trapping region were computed by integrating numerically Eq. (1.1) (Fig. 3 in [7]).

The theoretical boundary of stable trapping is thus a surface that separates two regions in which lie the mirror points of particles whose drift shells are either closed around the Earth or open, respectively. Whatever particles one finds mirroring and drifting inside the regions of quasi-trapping must have been injected from elsewhere; this is why one should expect low and fluctuating fluxes in the regions of quasi-trapping, as opposed to a larger, more smoothly varying flux in the region of stable trapping. The regions of quasi-trapping are limited on their outer side by the boundary of closed field lines, along which no adiabatic trapping is possible. An equivalent way of characterizing the limit of stable trapping is with the concept of a *drift loss cone*. At the minimum-B equator, this cone encompasses all pitch angles for which a particle mirrors inside the region of quasi-trapping. On the night side, the drift loss cone is oriented perpendicularly to the local field line; on the dayside, it is directed along the field line. Figure 3.13 shows the drift loss cones in addition with the "conventional" *bounce loss cones* along the field line.

Much of the preceding results obtained through numerical computer calculations using a model magnetospheric field can be described in a more approximate, but still physically meaningful, analytical way if one restricts the discussion to near-equatorial particles ($\cos\alpha \ll 1$) and uses a simple first-order analytical approximation of the magnetospheric field, as we did in Sect. 1.6. Neglecting any electric currents in the region to be examined (say, between 3 and 5 R_E during quiet times), we shall consider a field [8] derived from the following magnetic scalar potential (which gives the equatorial magnetic field (1.49) used in Sect. 1.6):

$$V(r,\theta,\phi) = R_E\left[-B_E\left(\frac{R_E}{r}\right)^2 + b_1\left(\frac{r}{R_E}\right)\cos\theta + \frac{1}{2}b_2\left(\frac{r}{R_E}\right)^2\sin(2\theta)\cos\phi\right] \tag{3.18}$$

The coefficients b_1 and b_2 are those of relations (1.50).

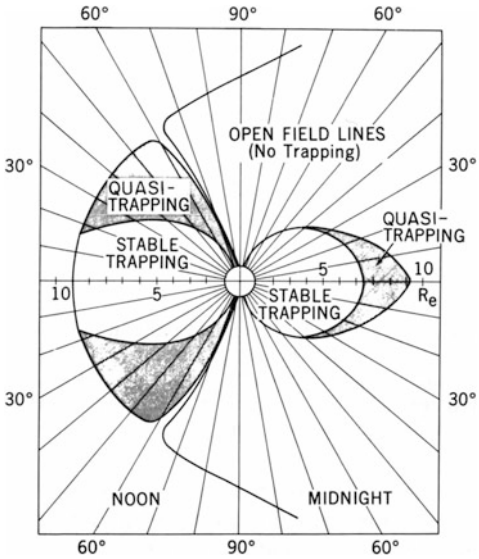

Fig. 3.12 Location of the quasi-trapping regions in the magnetosphere. Particles mirroring inside those regions are unable to complete a 360° drift around the earth. Those injected into the *left side* will be lost into the tail; those injected into the *right portion* will abandon the magnetosphere through the boundary on the dayside

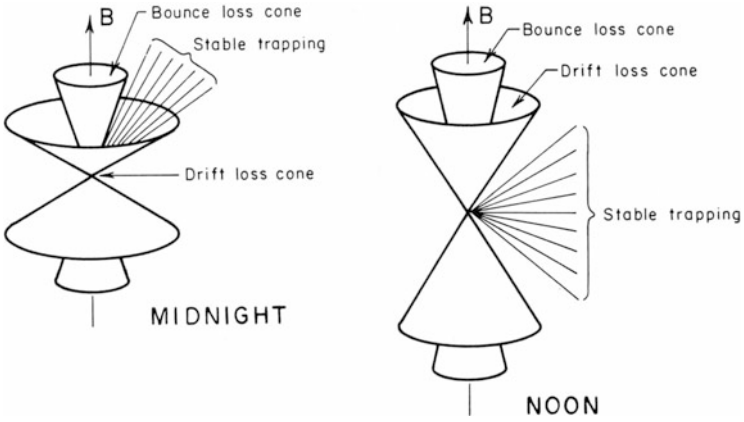

Fig. 3.13 Drift and bounce loss cones on the midnight and noon meridians

For convenience, we reproduce here the expression (1.49) for the magnetic field intensity B_0 on the equatorial plane:

$$B_0 = B_E \left(\frac{R_E}{r_0}\right)^3 \left[1 - \frac{b_1}{B_E}\left(\frac{r_0}{R_E}\right)^3 - \frac{b_2}{B_E}\left(\frac{r_0}{R_E}\right)^4 \cos\phi_0\right]$$

The quantity $a_0 = \partial^2 B/\partial s^2$ at a given equatorial point r_0, ϕ_0 can be (laboriously) calculated to obtain [9]:

$$a_0(r_0, \phi_0) = \frac{9B_E}{{r_0}^5}\left[1 + 2\frac{b_1}{B_E}\left(\frac{r_0}{R_E}\right)^3 + \frac{29}{8}\frac{b_2}{B_E}\left(\frac{r_0}{R_E}\right)^4 \cos\phi_0\right] \tag{3.19}$$

Combination of the two latter equations with (3.12) and (3.13) leads to the equation of the equatorial trace of the drift shell generated by a particle injected at point r_{0i}, ϕ_{0i} with a pitch angle cosine μ_{0i} ($\ll 1$):

$$r_0 = r_{0i} - \frac{R_E}{3}\frac{b_2}{B_E}\left(\frac{r_{0i}}{R_E}\right)^5 \left(1 - \frac{43}{18}{\mu_{0i}}^2\right)(\cos\phi_0 - \cos\phi_{0i}) \tag{3.20}$$

Compare this with (1.51); again, only the day-night asymmetry coefficient b_2 appears. An analysis of the case of equatorial particles ($\mu_{0i} = 0$) was given in Sect. 1.6.

According to (3.19) and for field parameters with $R_s = 10$, the quantity $a_0 = \partial^2 B/\partial s^2$ goes through zero at ${r_0}^* = 6.9\, R_E$ on the noon meridian ($\phi_0 = \pi$), becoming negative beyond. As one moves away from the noon meridian toward dawn or dusk, the critical distance ${r_0}^*$ increases and approaches the magnetospheric boundary. This obviously means that beyond a certain distance on the dayside, the $\theta = \pi/2$ plane *is no longer a minimum-B surface*. We already mentioned (page 59) that in that region, field lines attain their minimum B-value at two points situated at a certain finite latitude up and down from the equatorial plane. Again, since the field approximation used here starts breaking down at these distances, more realistic field models must be used to explore numerically the actual geometry of these *minimum-B pockets* and their effects on quasi-trapped particles.

Let us now examine Eq. (3.20) for $\mu_{0i} \neq 0$ (but still $\ll 1$). Drift-shell splitting becomes apparent. For a particle injected at midnight ($\phi_{0i} = 0$), the maximum radial deviation from a $\mu_{0i} = 0$ orbit occurs at noon ($\phi_0 = \pi$) and is given by

$$\Delta r_0 = r_0\big|_{\mu_{0i}=0} - r_0\big|_{\mu_{0i}\neq 0} = \frac{43}{27} R_E \frac{b_2}{B_E}\left(\frac{r_{0i}}{R_E}\right)^5 {\mu_{0i}}^2 \tag{3.21}$$

This is a positive quantity, which means that for particles with decreasing pitch angle at the midnight point (μ_{0i} increasing), drift shells will reach out farther on the dayside (see Fig. 3.10). For a particle injected at noon, the situation at midnight is reversed (the above equation has a minus sign); for smaller pitch angles at noon, the shells are displaced inward (toward the earth) at midnight. Notice the strong dependence on radial distance r_{0i}.

An interesting fact is the appearance of the combination $[1 - (43/18)\mu_{0i}{}^2]$ in (3.20). If we forget for a moment the condition $\mu_{0i} \ll 1$, it would mean that there is a "magic" pitch angle $\alpha^* = \arccos\sqrt{18/43} = 49.6°$, a sort of "universal constant" for a field of the type given by (3.18) (i.e., independent of the actual values of the parameters B_E, b_1, b_2 and of the coordinates r_0, ϕ_0), for which drift shells are azimuthally symmetric. As we shall see in Sect. 3.5, this characteristic is still retained if one uses more refined external field models and numerical shell tracing. One consequence is that whenever one measures particles with equatorial pitch angles of about 45°–50° (mirroring at about 23° geomagnetic latitude), it really is not necessary to specify the local time (or longitude) of the measurement, in spite of the asymmetry of the magnetic field. There is a simple physical explanation for the reversal of the shell asymmetry for a certain equatorial pitch angle. When $\mu_{0i} = 0$, particles follow *constant-B* contours, which approach the earth closest on the nightside. When $\mu_{0i} \to 1$, on the other hand, conservation of the invariant I can be shown to lead to the approximate constancy of the field-line *arc length* between mirror points. Since field lines are stretched out farther on the nightside, the corresponding shells also must reach out farther on the dayside because of the more compressed field lines there. Hence there must be an intermediate value of the pitch angle for which a shell is axisymmetric. The remarkable thing is that for magnetospheric-type field geometries this pitch angle depends very little on position and field parameters.

3.4 Effects of Internal Field Multipoles on Inner Magnetosphere Particle Shells; McIlwain's L-Value

In a pure dipole field, for reasons of longitudinal and latitudinal symmetry, drift shells are degenerate and there is no shell splitting—particles on one given field line, regardless of their pitch angle, will share the same field lines as they drift; only their drift speeds will differ, depending on pitch angle. Figure 3.14 reminds the reader of the symbols used. The fundamental sets of equivalent coordinates are $(\boldsymbol{r}, \lambda)$, (L, λ) or (B, L), with the parameter $L = r_0/R_E$ (r_0: equatorial point of a field line, R_E= Earth radius $\simeq$ 6,371 km). B_L is the B-value at the field line intersection with the Earth (or ionosphere) and B_E the value of B at the equatorial point on the Earth's surface (proportional to the Earth's dipole moment: $B_E = k_0\, R_E^{-3} \simeq 0.31$ Gauss). Of course, in three dimensions we must also include the longitude ϕ. For other planets or magnetized moons, just insert the corresponding values for R_E and B_E in what follows (e.g., for Jupiter, $B_J \cong 4.28$ Gauss).

The most important relationships between those variables for what follows (see Fig. 3.14) are:

$$L = \frac{r}{R_E}\frac{1}{\cos^2\lambda} \tag{3.22}$$

$$\cos^2\lambda_L = \frac{1}{L} \tag{3.23}$$

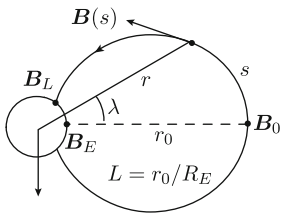

Fig. 3.14 Dipole field line parameters

$$B(L,\lambda) = \frac{B_E}{L^3}\frac{\sqrt{4-3\cos^2\lambda}}{\cos^6\lambda} = B_0\frac{\sqrt{4-3\cos^2\lambda}}{\cos^6\lambda} \tag{3.24}$$

$$B_L = B_E\sqrt{4-3/L} \tag{3.25}$$

$$A = B_E R_E/(L^2\cos\lambda) \quad \text{(in the direction of } +\phi) \tag{3.26}$$

$$ds = LR_E\cos\lambda\sqrt{4-3\cos^2\lambda}\,d\lambda \tag{3.27}$$

For the loss cone pitch angle at any B, L point we have

$$\mu_L^2 = 1 - \frac{B}{B_E}\frac{1}{\sqrt{4-3/L}} \tag{3.28}$$

Concerning the invariant I (2.37), there is a direct relationship with the L-value and B_m for a dipole field, based on the above relations:

$$I = LR_E\int_{-\lambda_m}^{+\lambda_m}\sqrt{1-\frac{B_E}{B_m L^3}\frac{\sqrt{4-3\cos^2\lambda}}{\cos^6\lambda}}\sqrt{4-3\cos^2\lambda}\cos\lambda\,d\lambda \tag{3.29}$$

The integral limits $\pm\lambda_m$ are the latitudes of the conjugate mirror points, obtainable from the inverse function of (3.24), $\lambda_m = \lambda_m(B_m L^3/B_E)$. Expression (3.29) is of the form

$$I = LR_E h\left(\frac{B_m L^3}{B_E}\right)$$

where h is a function for which there is no closed analytical expression; it must be determined by numerical integration. Cubing and multiplying both sides by B_m/B_E, we obtain for the inverse relationship

$$\frac{L^3 B_m}{B_E} = F\left(\frac{I^3 B_m}{R_E^3 B_E}\right) \tag{3.30}$$

This defines the L-parameter as a function of the pair I, B_m. The dimensionless function $y = L^3 B_m/B_E = F(x)$ of the dimensionless argument $x = I^3 B_m/(R_E^3 B_E)$ can be found in published tables (e.g., Appendix VI in [6]). Notice that (3.30) also represents the relation between I and B_m along a given field line or, in general, on a given L-shell in a dipole field.

In non-dipole trapping fields, one still can use relationship (3.30) to assign an L-value to a particle of given I and B_m values (calculated with the pertinent magnetic field model through (2.33) and (2.37), respectively):

$$L = \left(\frac{B_E}{B_m}\right)^{1/3} f\left(\frac{I^3 B_m}{R_E^3 B_E}\right) \tag{3.31}$$

The function f is the cubic root of F. However, defined in this way, L will *not* be constant along a field line as in the pure dipole field case, and it will lose its geometric meaning as the radial distance to the equatorial point of its guiding field line. Still, it is a useful parameter in "quasi-dipole" fields like the magnetosphere out to about $L = 7$ during quiet times, giving intuitive information about the radial extension of a drift shell. It is certainly more convenient than the original invariants I or the energy-dependent J, both of which of course vary strongly along a field line. For near-equatorial particles ($\mu_0 \to 0$, $I \to 0$) an expansion of function f in powers of its argument can be used. Using (3.12) we obtain to first order

$$L \simeq \left(\frac{B_E}{B_0}\right)^{1/3} + \mu_0^2 \left[\frac{1}{R_E}\sqrt{\frac{B_0}{a_0}} - \frac{1}{3}\left(\frac{B_E}{B_0}\right)^{1/3}\right] \tag{3.32}$$

This shows that for a pure dipole field L is independent of μ_0 because in that case $a_0 = \partial^2 B/\partial s^2 = 9(B_0/R_E^2)(B_E/B_0)^{-2/3}$ and the bracket is zero. For a dipole-like field with additional internal and external distortions, the definition of L in (3.31) still gives as *zeroth* approximation the radial distance in Earth radii to the equatorial point of a pure dipole field line with the same equatorial magnetic intensity B_0.

Just as velocity maps are a useful graphic instrument (e.g., Fig. 2.12) for the representation of field-aligned properties of trapped particles, so are $B - L$ maps for the representation of stably trapped particle properties on a drift shell in dipole-like fields. This "$B - L$ space" has a physical region bounded by the equatorial field $B_0(L) = B_E/L^3$ and the Earth intersection field $B_L(L) = B_E\sqrt{4 - 3/L}$ (3.25), as shown in Fig. 3.15. Drift shells map into vertical lines between the two curves; a given $B - L$ ring (e.g., a mirror point trajectory) maps into a point.

The Earth's internal magnetic field is not that of a pure dipole. Within about 4 R_E, where contributions from external currents can be neglected during magnetospherically quiet times, the internal geomagnetic field is indeed mainly dipolar with very slowly time-varying perturbations caused by irregularities in the electric current flow in the Earth's core and effects of the irregular distribution of matter with varying magnetic properties in the mantle and rocky crust. Solid earth geophysicists express the internal magnetic field above the earth surface as deriving from a scalar magnetic potential $V_m(r, \theta, \phi)$ where r, θ, ϕ are the geographic spherical coordinates of the point in question:

$$V_m(r, \theta, \phi) = R_E \sum_{n=1} \sum_{m=0}^{m=n} \left(\frac{R_E}{r}\right)^{n+1} \left(g_n^m \cos m\phi + h_n^m \sin m\phi\right) P_n^m(\theta) \tag{3.33}$$

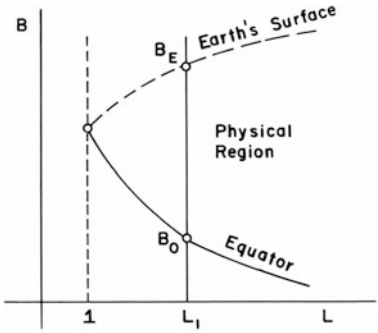

Fig. 3.15 The "good old" $B - L$ space and limiting curves defining the physically meaningful portion

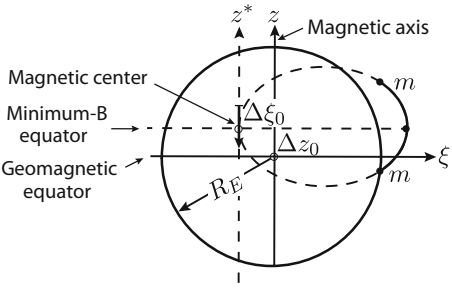

Fig. 3.16 Field line configuration of an off-center geomagnetic dipole

P_n^m are the associate Legendre functions, and the coefficients g_n^m and h_n^m are determined from data of the world network of magnetic observatories; they vary in time on a scale of decades to centuries (secular variation). The index n represents the multipole order, whose strength decreases with distance like $r^{-(n+1)}$. A more convenient and more physical form of representation of the internal field for space studies is obtained using the *geomagnetic coordinate system*, oriented in such a way that only one of the order $n = 1$ coefficients is non-zero ($g_1^0 \simeq 0.31$ Gauss; $g_1^1 = h_1^0 = h_1^1 \equiv 0$). In that system, the $n = 1$ dipolar axis is parallel to the polar axis. However, the dipole is not centered: the quadrupole terms with $n = 2$ and $m = 0, 1$ control the displacement of the main dipole away from the Earth's center. Since trapped particle drift shells are "frozen" into the magnetic field, their resulting geometric situation with respect to planet Earth is shown in Fig. 3.16 (exaggerated scale). In other words, the Earth sits off-center in the radiation belts (solid earth geophysicists would prefer a reverse statement!) with the result that it takes a bite out of them in a geographically limited region in the South Atlantic where mirror points come closest to the ionosphere, and loss cones widen,[5] and trapped particles may precipitate into the ionosphere (the area is called the

[5]This is precisely how James Van Allen and his group [10] discovered the radiation belt with the Explorer I and III satellites: a cosmic ray counter blacked out every time the satellites crossed the South Atlantic region. A careful analysis of the orbital points of saturation and recovery of the instrument and of the respective local magnetic field intensities led the scientists to the conclusion that the saturation had to be caused by a high flux of energetic particles trapped in the Earth's magnetic field (initially it was not clear whether the radiation was natural or consisting of trapped

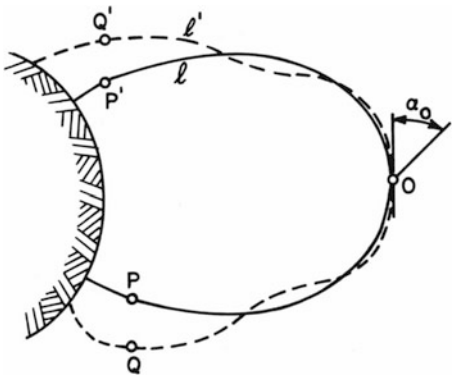

Fig. 3.17 Sketch of internal multipole-distorted field line (broken curve)

South Atlantic Anomaly). The upper limiting curve in Fig. 3.15 dips down in longitude-dependent fashion (more details below). Electrons, which drift from west to east, are wiped out in the anomaly at low L-shells and smaller pitch angles, but the flux recovers rapidly several tens of degrees longitude east of that area due to pitch angle scattering, which fills the emptied loss cones (in the early times this was called the "windshield wiper effect").

The multipole terms give rise to field distortions which decrease with distance faster than the dipole field. Thus the field distortion caused by them is much greater near the surface than further out in space. Let us imagine that we can switch these higher order multipoles on and off at will. If we start with a pure dipole field, the field line going through the equatorial point O is ℓ (Fig. 3.17). Now we turn on all higher multipoles. The field line through the same point O (which may no longer may be a minimum-B point) may look like the broken curve ℓ'. It will differ only very little from line ℓ near the equator, but may depart considerably from it near the earth.

A particle injected with a given pitch angle α_0 at O along the dipole field line ℓ will mirror at points P, P′ where the field intensity is $B_m = B_o/\sin^2\alpha_0$ (2.33). Its L-value will be given by (3.22). The same particle, injected with the same pitch angle along the field line ℓ' with all multipoles turned on, will mirror at the pair Q, Q′, different from P, P′ but where the field intensity is practically the same (different only to the extent that the *equatorial* field intensity B_0 differs a tiny bit from the original dipole value—see relation (2.33)). Will its I value be very different? Since the mirror points Q, Q′ are at positions different from P, P′, one may expect the I-value to be substantially different, too. Yet numerical calculations for the real geomagnetic field show that this is not the case. The reason for this near-equality is that the integrand $\sqrt{1 - B(s)/B_m}$ in (2.37) mainly contributes in the equatorial region where the multipole effect is strongly attenuated; toward the mirror points, where the multipole field distortion becomes more and more pronounced, the integrand decreases toward zero. The situation is quite different with the bounce period τ_b (2.34) or the half-bounce path length S_b (2.35) whose

beta decay electrons from fission products of secret high altitude explosions.) At nearly the same time, Sergei Vernov and his groupt at Moscow State University [11] saw the same effect happening to cosmic ray detectors on Sputnik satellites, but initially he attributed it to equipment failure.

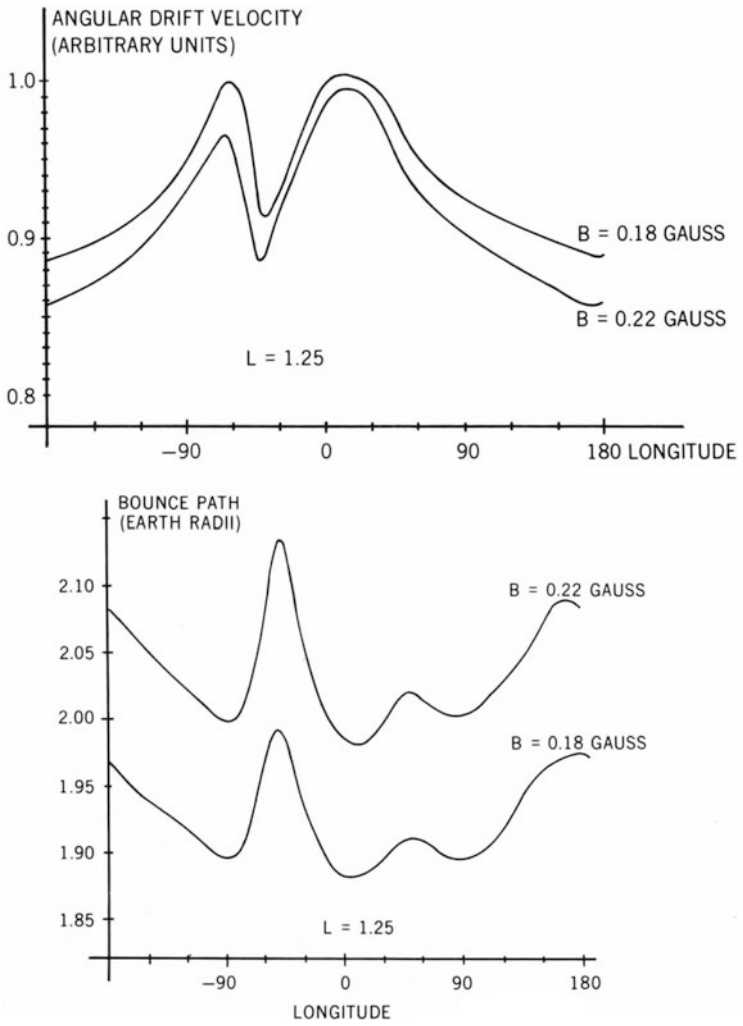

Fig. 3.18 Angular drift velocity (in arbitrary units) and bounce path S_b for particles at $L = 1.25$ and mirroring at $B_m = 0.18$ and 0.22 Gauss, respectively [12] (To obtain drift velocity in degrees/sec, multiply by factor given for Fig. 3.11)

integrands contain the same function but in the denominator. Its main influence now occurs in the region near the mirror points, causing bounce period and bounce path to differ appreciably from the dipole case (remember that a trapped particle always spends more time of its bounce oscillation near its mirror points than around the equatorial point!). Figure 3.18 shows the variation with longitude due to internal geomagnetic field multipoles of the bounce-average drift velocity and the bounce path, for particles at $L = 1.25$ mirroring near the Earth surface at $B_m = 0.18$ and 0.22 Gauss.

The above discussion leads to the following mutually equivalent consequences: (i) The L-value defined through dipole relation (3.31) (but computed using field values derived from (3.33)) will be nearly the same along a given field line in the real field as well as on the whole shell defined by particles mirroring on that field line. This is called *McIlwain's L value* [13]. (ii) All particles initially mirroring on a common field line will mirror on nearly coincident field lines at all other longitudes, generating a common drift shell; in other words, there is negligible shell splitting in the internal geomagnetic field. These facts also led to the use of another pair of invariant coordinates, the parameters R and Λ, solutions of the pair of equations

$$\begin{aligned} R &= L\cos^2\Lambda \\ B &= \frac{B_E}{R^3}\sqrt{4-\frac{3R}{L}} \end{aligned} \tag{3.34}$$

In these relations, B is the local B-value and L the solution of (3.31) for the local B, I values. For a pure dipole, of course $R = r/R_E$ and $\Lambda = \lambda$. Sometimes the parameter $\Lambda = \arccos\sqrt{(1/L)}$ is called "invariant latitude" and used for the description of high-latitude ionospheric phenomena. However, this is a misnomer: due to the effect of multipoles, $R = 1$ does *not* necessarily correspond to the Earth's surface (or, approximately, an ionospheric height). Only the simultaneous solutions of (3.34) are true invariant coordinates of a given point in space. Another warning: if used at high latitudes, even if at low altitude, the corresponding field lines are highly distorted by the external magnetospheric currents, and the use of any dipolar-like relationship (as in (3.31)) will be increasingly illegitimate.

3.5 Time-Changing Fields and the Third Adiabatic Invariant

Conservation of the adiabatic invariants M (1.26) and J (3.4) or I (2.37) hold only if fields and external forces change very little during a cyclotron period (2.2) and a bounce period (3.8), respectively. In this chapter we shall examine explicitly the effect of *time variations* of the magnetic field under certain limiting conditions on particle drift shells and energy.

Let us imagine a trapping magnetic field configuration whose time variations can be turned on and off, at our own will. We first impose the restriction of dealing only with particles which during static conditions are on closed shells (i.e., stably trapped whenever time variations are turned off). In this situation, the drift motion represents the third periodicity of the general equation of motion (1.1).

Quite often one is not interested in the actual drift phase of a particle; in such a case the drift motion may be averaged out. One can still investigate the configuration and time-change of the "bare" drift shell without worrying about where on that drift shell the particle is located at any given time. This is physically analogous to averaging out the cyclotron phase and working with the guiding center, or to averaging out the bounce motion and working with the guiding field line, without specifying the cyclotron or bounce phases, respectively. The quantity

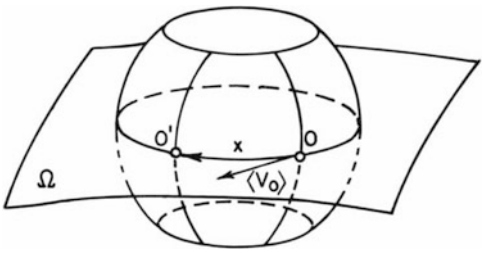

Fig. 3.19 Parameters of the drift shell of a positive particle in the earth's field

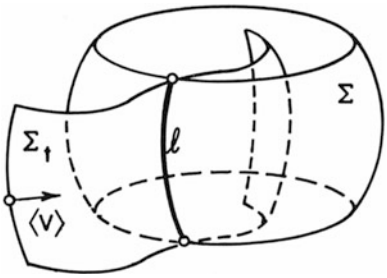

Fig. 3.20 Illustrating the concept of instantaneous guiding drift shell in a time-dependent field

$$\tau_d = \oint \frac{d\ell}{\langle V_0 \rangle} \tag{3.35}$$

is the *drift period* ($\langle V_0 \rangle$ is the bounce-average drift velocity (3.7)). The integral is computed along a closed line on the drift shell (Fig. 3.19) under *static* conditions (with all time variations turned off). In (3.35) $d\ell$ is the element of arc length of the intersection of the drift shell with the reference surface Ω (usually the minimum-B surface). Whereas $\langle \boldsymbol{V}_0 \rangle$ and the integration path depend on the reference surface, τ_d does not. Under the conditions (2.2) and (3.8) for conservation of M and J, we have $\tau_c \ll \tau_b \ll \tau_d$; any field time variation $\dot{B}$ that fulfills the condition

$$\tau_d \ll \frac{B}{\dot{B}} \tag{3.36}$$

may be called a "fully adiabatic" change. The other restrictive condition which we impose for our discussion in this section is that no non-electromagnetic forces act on the particle.

We now switch on a time variation of the magnetic field. A force will appear, given by the *induced electric field* associated with the time-dependent magnetic field. This induced electric field E_{ind} causes an additional drift (1.34) which drives the particle out of its initial shell. During the interval of transient conditions the particle's drift shell may not be closed. Consider such a transient drift shell Σ_t as shown in Fig. 3.20. At a given time t the particle's guiding field line is $\boldsymbol{\ell}$. If at that instant we turn off the time variation and "freeze" the magnetic field configuration, we may again have the particle following a static closed drift shell Σ. For each time and position on the transient shell we can

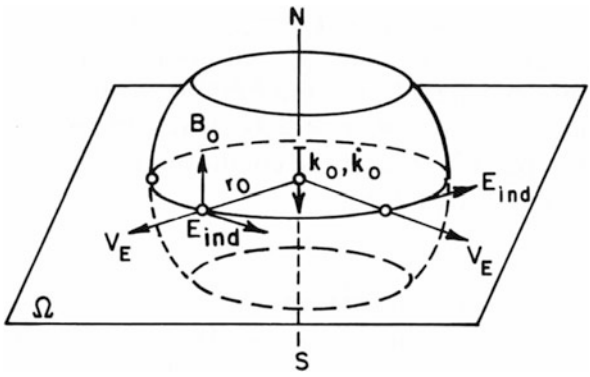

Fig. 3.21 Induced electric field in a dipole field of increasing dipole moment k_0

thus define an associated closed shell, which is the one that would be generated by the particle if we were to turn off all time variations at that instant. We call this static shell by analogy the *guiding drift shell*. The drift period of the particle on the guiding drift shell may be called the *instantaneous drift period* of the particle. During static conditions the guiding drift shell represents the actual drift shell of a particle, just as a guiding field line represents the actual portion of a field line on which a particle is momentarily bouncing. When the field changes, a particle is transferred from one guiding drift shell to another by the drift caused by the induced electric field.

For instance, if we have a dipole field and gradually increase the dipole moment k_0, we will induce an azimuthal electric field of the direction as shown in Fig. 3.21 (using Faraday's law, $E_{ind} = (dk_0/dt)\, r^{-2}$). This electric field produces an *outward* drift (for positive *and* negative charges) and the guiding drift shell will inflate. Likewise, a decrease of the dipole moment causes guiding drift shells to contract. A change in drift shell is, of course, accompanied by a change in particle energy. In order to compute this change, we envisage Eq. (2.26) and average it over a bounce period (in absence of external forces):

$$\left\langle \frac{dT}{dt} \right\rangle_b = M \left\langle \frac{\partial B}{\partial t} \right\rangle_b + q \langle \boldsymbol{V} \cdot \boldsymbol{E}_{ind} \rangle_b$$

As to the second term $\langle \boldsymbol{V} \cdot \boldsymbol{E}_{ind} \rangle_b$, we first notice that it is equal to $\langle \boldsymbol{V}_{GC} \cdot \boldsymbol{E}_{ind} \rangle_b$, in view of the fact that there are no external forces other than $q\boldsymbol{E}_{ind}$ and that the drift component $(\boldsymbol{E}_{ind} \times B)/B^2$ caused by $\boldsymbol{E}_{ind}$ is perpendicular to it ($\boldsymbol{V}_{GC}$ is the gradient-curvature drift (2.17)). It can be shown (on similar lines as for (3.6)) that

$$\langle \boldsymbol{V}_{GC} \cdot \boldsymbol{E}_{ind} \rangle_b = \langle \boldsymbol{V}_{GC0} \rangle_b \cdot \boldsymbol{E}_{ind0}$$

The subindex 0 refers to the minimum-B point of the guiding field line. We thus have, finally,

$$\left\langle \frac{dT}{dt} \right\rangle_b = M \left\langle \frac{\partial B}{\partial t} \right\rangle_b + q \langle \boldsymbol{V}_{GC0} \rangle_b \cdot \boldsymbol{E}_{ind0} \tag{3.37}$$

The first term represents what has been called the *gyro-betatron* acceleration effect (see also Sect. 2.2), because it gives the power delivered by the induced electric field force to the particle in its cyclotron motion mode. The second term represents the *drift-betatron*, i.e., the power delivered by the induced electric field to the particle's gradient-B drift mode.

In order to find the actual drift shell of a particle in a time-dependent magnetic field, we have to integrate the bounce-average total drift velocity (3.7), in which $\boldsymbol{E}_0 = \boldsymbol{E}_{ind}$, and make use of the conservation of M and $K = I\sqrt{B_m}$. The main practical problem lies with the determination of $\boldsymbol{E}_{ind}$, which has to be computed numerically. Assuming zero field-aligned electric fields and that the magnetic field lines are rooted into the ionosphere (frozen-in field lines, Sect. 5.5), one reasonable way is to (i) trace the field line from the minimum-B surface point $\boldsymbol{P}$ (at which $\boldsymbol{E}_{ind}$ is wanted) to the ionosphere; (ii) let the external magnetospheric field change in time Δt; (iii) re-trace back from the fixed ionospheric point to the new minimum-B point $\boldsymbol{P}' = \boldsymbol{P} + \boldsymbol{\Delta r}$; (iv) take the vector $\boldsymbol{\Delta r}/\Delta t\, B_0$ as a good approximation of $\boldsymbol{E}_{ind}$. As examples, consider two extreme cases.

(i) If the time variation is *fast* with respect to the drift period (but still slow compared to the bounce period, $\tau_b \ll B/\dot{B} \ll \tau_d$), the induced electric field drift will dominate over the gradient-curvature drift, and the particle will be driven mainly by the former during the transient interval. The drift velocity will be that of the guiding field line or, which is equivalent, the particle's guiding field line will be "frozen" into the changing magnetic field configuration and move with the latter. The acceleration (or deceleration) is then of "gyro-betatron" type (first term of (3.37)). If the time variation persists long enough, the particle may acquire sufficient energy to let the gradient-curvature drift take over and move it away from the initial moving field line. As a matter of fact, this represents a fundamental acceleration mechanism of radiation belt particles during geomagnetic substorms during which field lines are being "pulled from the tail towards the earth" in the midnight meridian region. Low energy particles are thus carried with these field lines by the induced electric field drift and accelerated by the gyro-betatron until the gradient-curvature drift takes over, ejecting them from their guiding field line and the acceleration region, eventually placing them on closed shells (stably trapped orbits). For the same reason, sudden asymmetric compressions of the magnetosphere caused by brusque variations of the dynamic pressure of the solar wind, can cause acceleration of particles found on the dayside and their placement into trapped orbits (see later). It should also be clear that, unless there is azimuthal symmetry both in drift shells and $\partial \boldsymbol{B}/\partial t$, particles belonging to the same drift shell but with different drift phases (e.g., longitude or arc position of their equatorial crossings) will in general not end up on a common drift shell as the time variation goes on—a fact that can lead to radial diffusion (see Chap. 4).

(ii) The other extreme case is given by time variations that are fully adiabatic, i.e., *very slow* compared to a drift period. In such a case a *third conservation theorem* applies, which can be conveniently used in numerical computations: The magnetic flux encompassed by the guiding drift shell of a particle remains constant, provided condition (3.36) is fulfilled:

$$\Phi = \oint \boldsymbol{A}_0 \cdot \boldsymbol{d\ell} = \text{const.} \tag{3.38}$$

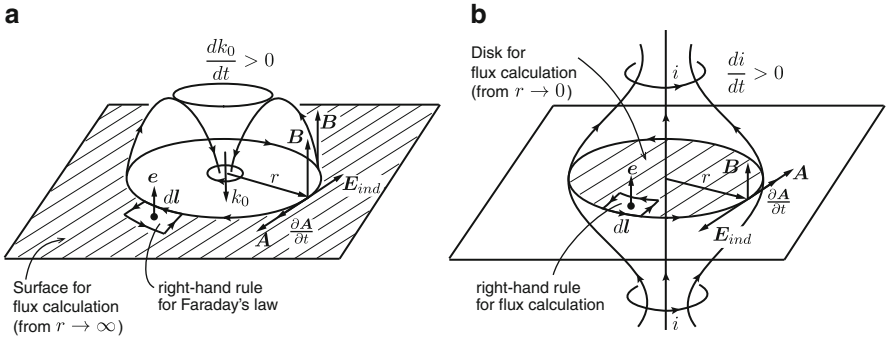

Fig. 3.22 Definition of the third invariant (flux Φ) for a dipole-like (**a**) and mirror machine-like (**b**) closed drift shell. In (**a**), because of the singularity at the origin, the flux Φ must be calculated over the surface lying outside the drift shell

$\boldsymbol{A}_0$ is the magnetic vector potential and the integral is carried out along a curve which lies in the (time-frozen) guiding drift shell of the particle (e.g., intersection with the minimum-B surface; see Fig. 3.22). It is important to remind the reader that in a static situation in absence of any external forces, a drift shell is independent of the particle's kinetic energy and fully determined by just two invariants M (or B_m) and I (e.g., relations (3.9) and (3.10)). Φ is *not* an independent parameter under these conditions. For a time-dependent magnetic field, B_m and I are no longer invariant, and a shell must be determined by the general invariants M, J (or K in absence of field-aligned electric fields) and Φ, as we shall describe below.

The demonstration of the conservation theorem for Φ is lengthy [1, 14].[6] In Appendix A.3 we give a simplified demonstration limited to equatorial (90°) pitch angle particles. It is very important to emphasize that Φ is defined and computed for the *guiding* drift shell (i.e., holding the field constant and finding out what closed shell would be generated by the particle), and *not* for the actual drift shell of the particle during transient conditions. However, in view of the condition of slow changes (3.36), the actual drift shell will differ only very little from the instantaneous guiding drift shell. Indeed, we may picture this situation as having the particle drifting many times around a closed shell while the latter is slowly changing its shape. Note that if (3.36) holds for a given class of particles, because of the energy-dependence of the gradient-curvature drift this may not be true for other particles on the same initial shell. For a given scale $B/\dot{B}$ of time variation, the lower the particle energy, the more likely it is that condition (3.36) will be violated. On the other hand, particles of the same kind but different drift phases starting on a common drift shell may end up on different drift shells as the time-variation goes on. In Appendix A.3 we show under what conditions these particles do reassemble

[6] Or we may just refer again to analytical mechanics (see footnote on page 10) and remark that in the canonical path integral for the cyclic drift motion $J_d = \oint (\boldsymbol{p} + q\boldsymbol{A}) \cdot \boldsymbol{dl}$, the first term is zero to first order (the average $\boldsymbol{p}$ vector is just $m\boldsymbol{V}_D$), so that what remains is $J_d = \oint q\boldsymbol{A} \cdot \boldsymbol{dl} = q\Phi =$ const.!

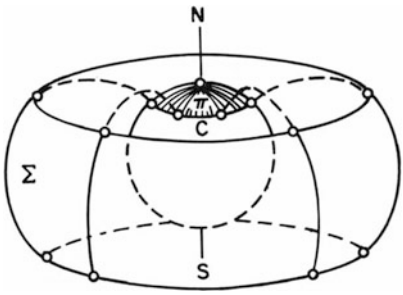

Fig. 3.23 Projection of a drift shell Σ onto the polar cap (π) along its magnetic field lines

on one common drift shell (integer multiples of τ_d!). In those cases the conservation of Φ is true only in *drift-average* terms. This is equivalent to what happens in shell splitting (Sect. 3.3): particles with different pitch angles on a common initial guiding field line will all pass through that same initial field line at integer multiples of drift time.

For a dipole field the magnetic flux encompassed by a particle shell defined by the parameter L (3.22) (Fig. 3.22) is given in absolute value by

$$\Phi = \frac{2\pi k_0}{r} = \frac{2\pi B_E {R_E}^2}{L} = \frac{1.953}{L} \text{ Gauss} R_E^2 \tag{3.39}$$

For other magnetized planets, the corresponding value of B_E must be used. It is important to note that in this case and all dipole-like field geometries, Φ is equal to the flux $\int \boldsymbol{B} \cdot \boldsymbol{dS}$ integrated over the portion of the equatorial surface *outside* of the intersection O of the shell with Ω. This obliges us to be careful with the sense of integration of the vector potential in the determination of the flux (3.38).

For a more complex field geometry the integral (3.38) has to be carried out numerically. This requires knowledge of the vector potential $\boldsymbol{A}$. A more practical way for the closed field lines in the Earth's magnetosphere is to find the intersection C of a series of shell field lines with the earth's surface (Fig. 3.23), and to numerically compute the flux

$$\Phi = \int_{\pi} \boldsymbol{B} \cdot \boldsymbol{dS}$$

over the polar cap Π, using the earth's known *surface* field B_s in that cap. For most magnetospheric models it will be sufficient to use the dipole approximation for B_s. Calling $\lambda_C(\phi)$ the dipole latitude of the intersection C at a given longitude ϕ, the shell flux will be, in absolute value (using (3.24)):

$$\Phi \cong 2B_E {R_E}^2 \int_0^{2\pi} d\phi \int_{\lambda_C(\phi)}^{\pi/2} \cos\lambda \sin\lambda d\lambda = B_E {R_E}^2 \int_0^{2\pi} \cos^2[\lambda_C(\phi)] d\phi \tag{3.40}$$

A convenient "recipe" to evaluate numerically the third invariant in the outer magnetosphere is therefore: (i) Trace the particle's guiding shell by methods given in Sect. 3.2; (ii) Find the intersection dipole latitude $\lambda_C(\phi)$ as a function of longitude for a set of shell field lines tracing them down to the earth's surface; (iii) Integrate numerically (3.40).

Let us show how the third adiabatic invariant can now be used to determine the fate of a (non-relativistic) particle trapped in a time-dependent field subject to the adiabatic condition (3.36), in absence of external forces. We start with a static field and a non-relativistic particle of energy T, having invariant parameters I, B_m. As long as the field remains static, the particle will drift on a closed shell of flux Φ given by (3.38) or (3.40). We now switch on the time variations. The particle will drift away from the initial shell surface. If the time variation ceases after an interval Δt, the particle will again be found on a closed, static shell. The flux through the shell in this final state must be equal to the flux through the initial shell. But the energy of the particle T^* and its parameters I^* and B_m^* will have changed—yet $M = T^*/B_m^*$ and $K = I^*\sqrt{B_m^*}$ must be the same as in the initial state. Therefore, to determine the final shell, one proceeds as follows: (i) pick a (reasonable) pair of values I^* and B_m^* that satisfy $I^*\sqrt{B_m^*} = I\sqrt{B_m}$; (ii) trace the shell in the final field configuration for these two values, as explained on page 63; (iii) find the flux Φ^* (3.40) through this shell; (iv) iterate steps (ii) and (iii), changing I^* and B_m^* as many times as necessary until the final Φ^*-value is equal to the initial one ($\pm$ prefixed error); (v) compute the particle's final energy from $T^* = (T/B_m)B_m^*$.

Adiabatic time changes satisfying the condition (3.36) are reversible: when the field configuration comes back to the initial state, all particles come back to their initial drift shells. This follows directly from the conservation of Φ. For non-adiabatic time variations this is no longer true, even if M and J are still conserved. It is important to note that *in absence of external forces* shell behavior in an adiabatic time-dependent field is *independent of particle energy, mass and charge* (as happens in the static case). Theorem (3.38) holds even if external forces are acting. Moreover, it holds when B is static but the external forces are adiabatically time-dependent. One final remark on condition (3.36): if the time-dependent magnetic field is azimuthally symmetric *at all times* (i.e., symmetric field with symmetric perturbations), Φ happens to be conserved even if the adiabatic condition is *not* fulfilled.

We are now in the position to create an ideal, truly invariant *reference representation* of particles found stably trapped in any non-symmetric magnetospheric field configuration. For that purpose, we need a sophisticated numerical model of the magnetic field, with parameters that can be conveniently adjusted to reproduce quantitatively the trapping magnetic field configuration of the moment (e.g., based on some real-time magnetic field measurements in strategic regions of the magnetosphere). Suppose we have such a sophisticated model on hand. For a given particle of energy T, pitch angle α and position $\boldsymbol{r}$, the model can be used to determine numerically the local magnetic field intensity B and the particle's invariant parameters M, K and, through shell tracing, Φ. Now we imagine turning off very slowly all external field sources (e.g., boundary and neutral sheet currents) and, if we are close to the Earth's surface, also the internal multipoles, leaving just the field of a central pure dipole of moment $k_0 = B_E R_E^3$. The particle, while conserving the values of its adiabatic invariants, will end up in a beautifully symmetric dipole drift shell defined by what we can call the *adiabatic reference parameters* and designate as "L-star" L^* and "B-star" B_m^*, respectively.[7] The particle kinetic energy, of course, will also be different, T^*.

[7] In the literature L^* has sometimes been called the "Roederer L-value" to distinguish it from the "McIlwain L-value" (3.30).

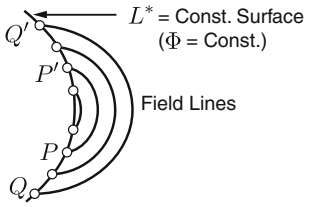

Fig. 3.24 Mirror points on different field lines for which trapped particles have the *same* L^* value

The adiabatic conservation theorems allow us to calculate the values of these reference parameters. The determination of L^* is straightforward, based on relation (3.39):

$$L^* = \frac{2\pi B_E {R_E}^2}{\Phi} \tag{3.41}$$

Once we have L^*, we can use dipole relation (3.31) to determine B_m^* by replacing on the right side the I^*-value by $I^* = K(B_m^*)^{-1/2}$ and solving the functional relationship for B_m^*. The particle energy is then obtained through the conservation of M: $T^* = T(B_m^*/B_m)$ (relativistically, we would obtain for the momenta $p^{*2} = p^2(B_m^*/B_m)$). If we are using the transformation to a stationary reference dipole field for standard flux mapping purposes, also the *flux values must be transformed*; this will be addressed in the next chapter. Finally, it is important to be well aware of the fact that a surface of constant L^* (see Fig. 3.24) represents neither a particle shell nor a collection of field lines. It simply gives the locus of all mirror points $P, P' \ldots Q, Q' \ldots$ of particles whose drift shells have the same Φ-value. Transforming adiabatically into a pure dipole field, all mirror points shown in this figure will assemble on one single dipole field line and shell surface (with different energies though, if initially they all had the same). Conversely, the L^* value (or Φ) will vary along a given field line in the real field because particles mirroring at different points of that field line generate different drift shells with different Φ values.

We can figure out the differences in Φ or L^* values. Let us use the same approximations for the field and other field-related quantities for near-equatorial particles as in Sects. 1.6, 3.2 and 3.3 (particularly (3.19) and (3.20)), to obtain following approximate expression for the L^* value of a particle injected at the equatorial point r_0, ϕ_0 with a pitch angle close to 90° ($\mu_0 \ll 1$):

$$L^*(r_0, \phi_0, \mu_0) \simeq \frac{r_0}{R_E}\left(1 + \frac{1}{2}\frac{b_1}{B_E}\left(\frac{r_0}{R_E}\right)^3 - \frac{1}{3}\frac{b_2}{B_E}\left(\frac{r_0}{R_E}\right)^4\left(1 - \frac{43}{18}\mu_0^2\right)\cos\phi_0\right) \tag{3.42}$$

Note the effects of magnetospheric compression (b_1 term) and day-night asymmetry (b_2 term).

The quantity

$$\sigma_A = -\frac{1}{3}\frac{b_2}{B_E}\left(\frac{r_0}{R_E}\right)^5\left(1 - \frac{43}{18}\mu_0^2\right)\cos\phi_0 \tag{3.43}$$

may be called the shell asymmetry parameter. According to (1.50) any changes of the stand-off distance R_s will lead to changes in the radial parameter L^*. It is important to interpret Eq. (3.42) correctly: it gives the approximate L^* value of a particle injected at an *initial* equatorial point with an *initial* pitch angle under magnetospheric field conditions given by the constants b_1 and b_2. If these constants change *adiabatically* (slowly compared to a drift period), the value of L^* will remain constant (conservation of Φ!) but the drift shell will change. To obtain the new drift trace one has to solve (3.43) for $r_0 = r_0(\phi_0)$ and constant L^* given by the initial conditions. For fast changes of b_1 and b_2, the drift-average of the change in L^* (only the constant b_2 will contribute) will give a measure of the effect on third invariant changes (see next chapter).

The dimensionless quantity

$$\sigma_S = \frac{\partial^2 L^*}{\partial \mu^2} = \frac{43}{54} \frac{b_2}{B_E} L^{*5} \cos \phi_0 \tag{3.44}$$

can be taken as a quantitative measure of shell splitting (second derivative, because the first derivative is zero on the equator). Only in the case of shell degeneracy, i.e., for azimuthally symmetric fields, will L^* and Φ be constant along a field line and $\sigma = 0$. Notice that $\sigma_S < 0$ on the day side ($\cos \mu < 0$) and positive on the night side. In other words, particles mirroring at higher latitude (i.e., with smaller equatorial pitch angles) on the noon/midnight field line, have smaller/larger L^*-values (larger/smaller third invariant Φ). This is directly related to the inward/outward reversal of shell splitting for noon/midnight field line particles (see Figs. 3.9 and 3.10). The drift-average of σ_S^2 is a good measure of the influence of the general state of the magnetosphere (represented by the parameter R_s) and the asymmetry of drift shells and its relation to drift shell splitting. As such it plays a role in radiation belt diffusion. Taking into account (1.50) we can establish the following proportionality (the actual factors of proportionality are magnetospheric model dependent):

$$\langle \sigma_S^2 \rangle \sim R_s^{-8} L^{10} \tag{3.45}$$

Notice the strong dependence on the stand-off distance of the magnetospheric boundary and the even stronger dependence on the radial shell parameter L.

Turning back to the general case of off-equatorial particles, one important remark. We often talk about the L^*-value of this or that point $\boldsymbol{r}$ in real 3-D space. One has to have clearly in one's mind what is meant by that, because, in general, the drift shell of a particle will depend on its energy. Can we even talk of the L^*-value "of a point" (Fig. 3.24) in such a case? *Yes we can*—provided we define it clearly: it is the L^*-value of a particle *mirroring at that point* when the *magnetic field is held constant in time*, and when *all electric fields have been turned off*.

Finally, Fig. 3.25 gives an example for particles with a series of different pitch angles detected at several different local times in synchronous orbit ($r = 6.6\, R_E$), using a magnetospheric field model for quiet time [15]. The picture clearly shows the portions of invariant reference B^*-L^* space scanned by such detectors. In a pure dipole field, each detector would just "see" one point in B, L space; there would be no local-time

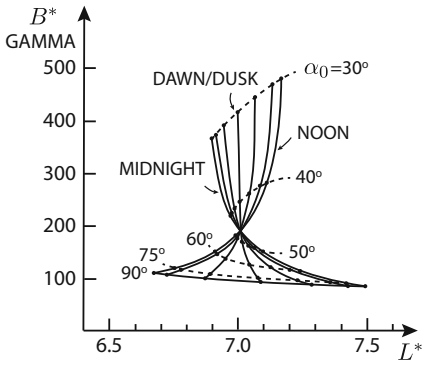

Fig. 3.25 Coordinates in invariant $B^* - L^*$ space (see text) of the particles registered with a directional detector in synchronous orbit

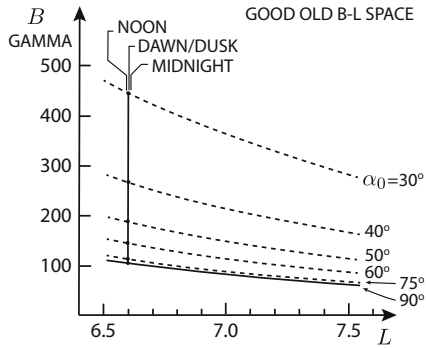

Fig. 3.26 Same as Fig. 3.25, in McIlwain's $B - L$ space

effect, and the region sampled would just be a straight vertical line (Fig. 3.26). For increased magnetospheric compression, the pattern in the figure spreads out in L^* coverage. Notice in Fig. 3.25 that for pitch angles around 45°–50°, the whole local-time asymmetry disappears and its effect reverses. This is related to what we have mentioned on page 72 in connection to shell splitting and its reversal at what we have called a "magic" pitch angle, because it barely changes as a function of specific parameters governing the external current contributions in the magnetospheric model. We shall come back to this invariant mapping procedure in the next chapter.

References

1. T.G. Northrop, *The Adiabatic Motion of Charged Particles* (Interscience Publishers, New York, 1963)
2. D.P. Stern, Euler potentials. Am. J. Phys. **38**, 494–501 (1970)
3. K. Min, J. Bortnik, J. Lee, A novel technique for rapid L* calculation using UBK coordinates. J. Geophys. Res. **118**, 192–197 (2013)
4. E.C. Stone, The physical significance and application of L, B_0, and R_0 to geomagnetically trapped particles. J. Geophys. Res. **68**, 4157–4166 (1963)
5. D.J. Williams, G.D. Mead, Nightside magnetosphere configuration as obtained from trapped electrons at 1100 kilometers. J. Geophys. Res. **70**, 3017–3029 (1965)

6. J.G. Roederer, *Dynamics of Geomagnetically Trapped Radiation* (Springer, New York, 1970)
7. K. Min, J. Bortnik, J. Lee, A novel technique for rapid L^* calculation: algorithm and implementation. J. Geophys. Res. **118**, 1912–1921 (2013)
8. G.D. Mead, Deformation of the geomagnetic field by the solar wind. J. Geophys. Res. **69**, 1181–1195 (1964)
9. J.G. Roederer, M. Schulz, Effect of shell splitting on radial diffusion in the magnetosphere. J. Geophys. Res. **74**, 4117–4122 (1969)
10. J.A. Van Allen, G.H. Ludwig, E.C. Ray, C.E. McIlwain, Observations of high intensity radiation by satellites 1958 Alpha and Gamma. Jet Propuls. **28**, 588–592 (1958)
11. S.N. Vernov, A.E. Chudakov, E.V. Gorchakov, J.L. Logachev, P.V. Vakulov, Study of the cosmic-ray soft component by the 3rd Soviet Earth Satellite. Planet. Space Sci. **1**, 86 (1959)
12. J.G. Roederer, J.A. Welch, J.V. Herod, Longitude dependence of geomagnetically trapped electrons. J. Geophys. Res. **72**, 4431–4447 (1967)
13. C.E. McIlwan, Magnetic coordinates. Space Sci. Rev. **5**, 585–598 (1966)
14. T.G. Northrop, E. Teller, Stability of the adiabatic motion of charged particles in the Earth's field. Phys. Rev. **117**, 215–225 (1960)
15. J.G. Roederer, Geomagnetic field distortions and their effects on radiation belt particles. Rev. Geophys. Space Phys. **10**, 599–630 (1972)